Available online at www.sciencedirect.com

ScienceDirect

Geochimica et Cosmochimica Acta 132 (2014) 94–100

Geochimica et Cosmochimica Acta

www.elsevier.com/locate/gca

Partitioning of Si and platinum group elements between liquid and solid Fe–Si alloys

G. Morard [a,b,*], J. Siebert [a,b], J. Badro [b,c]

[a] Institut de Minéralogie, de Physique des Matériaux, et de Cosmochimie (IMPMC) Sorbonne Universités – UPMC Univ Paris 06, UMR CNRS 7590, Muséum National d'Histoire Naturelle, IRD UMR 206, 4 Place Jussieu, F-75005 Paris, France

[b] Institut de Physique du Globe de Paris, Sorbonne Paris Cité – Université Paris Diderot, UMR CNRS 7154, F-75005 Paris, France

[c] Earth and Planetary Science Laboratory, Ecole Polytechnique Fédérale de Lausanne, Lausanne, Switzerland

Received 9 September 2013; accepted in revised form 31 January 2014; Available online 20 February 2014

Abstract

Crystallization of the Earth's inner core fractionates major and minor elements between the solid and liquid metal, leaving physical and geochemical imprints on the Earth's core. For example, the density jump observed at the Inner Core Boundary (ICB) is related to the preferential partitioning of lighter elements in the liquid outer core. The fractionation of Os, Re and Pt between liquid and solid during inner core crystallization has been invoked as a process that explains the observed Os isotopic signature of mantle plume-derived lavas (Brandon et al., 1998; Brandon and Walker, 2005) in terms of core–mantle interaction. In this article we measured partitioning of Si, Os, Re and Pt between liquid and solid metal. Isobaric (2 GPa) experiments were conducted in a piston-cylinder press at temperatures between 1250 °C and 1600 °C in which an imposed thermal gradient through the sample provided solid–liquid coexistence in the Fe–Si system. We determined the narrow melting loop in the Fe–Si system using Si partitioning values and showed that order–disorder transition in the Fe–Si solid phases can have a large effect on Si partitioning. We also found constant partition coefficients (D_{Os}, D_{Pt}, D_{Re}) between liquid and solid metal, for Si concentrations ranging from 2 to 12 wt%. The compact structure of Fe–Si liquid alloys is compatible with incorporation of Si and platinum group elements (PGEs) elements precluding solid–liquid fractionation. Such phase diagram properties are relevant for other light elements such as S and C at high pressure and is not consistent with inter-elemental fractionation of PGEs during metal crystallization at Earth's inner core conditions. We therefore propose that the peculiar Os isotopic signature observed in plume-derived lavas is more likely explained by mantle source heterogeneity (Meibom et al., 2002; Baker and Krogh Jensen, 2004; Luguet et al., 2008).

1. INTRODUCTION

Silicon is potentially one of the main light elements in the Earth's core due to its large abundance in the solar system and its high solubility in the metallic phase during Earth's differentiation (Takafuji et al., 2005; Siebert et al., 2013). It has also been shown that Fe-Ni-Si alloys are the only ones that have elastic properties that match those of the inner core (Badro et al., 2007; Antonangeli et al., 2010). The Fe–Si phase diagram is quite different than that of Fe–S or Fe–C: it shows an enhanced solubility of Si in solid Fe and displays solid solution behavior under Earth's core conditions, and a partitioning between solid and liquid expected to be close to unity at the Inner Core Boundary (ICB) (Alfè et al., 2002). However, an experimental determination of this Si partitioning is required for comparison

* Corresponding author at: Institut de Physique du Globe de Paris, Sorbonne Paris Cité – Université Paris Diderot, UMR CNRS 7154, F-75005 Paris, France. Tel.: +33 1 44 27 52 22.
E-mail address: guillaume.morard@impmc.jussieu.fr (G. Morard).

http://dx.doi.org/10.1016/j.gca.2014.01.044
0016-7037/

with ab initio calculations. Furthermore, the amount of light elements released in the liquid phase during inner core crystallization is quite important to model solutal convection in the Earth's core, potentially the main driving force of the Earth's magnetic field (Kutzner and Christensen, 2000).

Liquid metal infiltration from the outer core into minerals of the lower mantle has been postulated based on the chemical composition of mantle plume-derived lavas from oceanic islands which could directly sample the Core Mantle Boundary (CMB) (Brandon et al., 1998; Brandon and Walker, 2005). In detail, the coupled enrichment in $^{187}Os/^{188}Os$ and $^{186}Os/^{188}Os$ relative to upper mantle materials is attributed to the development of elevated Re/Os and Pt/Os in the outer core during inner core crystallization. The assignment of such isotopic anomalies to an outer core component has been strongly debated, as this Os isotopic signature could alternatively be produced by recycling of crustal materials or source mantle regions having experienced metasomatism (Meibom et al., 2002, 2004; Luguet et al., 2008; Day et al., 2010). Further objection to the core–mantle exchange model has been raised from the absence of W isotope anomaly in these mantle plume-derived lavas (Schertsen et al., 2004).

The core-mantle exchange model requires higher liquid–solid metal partitioning coefficients for Pt, Re and Os than those measured for pure Fe crystallization (Brandon et al., 2003). Over the last decade numerous high pressure and high temperature experimental studies have focused onto constraining the partitioning of Re, Pt and Os between liquid and solid metal for different Fe light element alloy systems (Chabot et al., 2006, 2011; Van Orman et al., 2008; Hayashi et al., 2009). Previous studies have considered the effect of sulfur and carbon as potential light elements in the core and partitioning values for Pt, Re and Os that were not consistent with the Os isotopic values required by the core–mantle exchange hypothesis. These partition coefficients depend mainly on the light element content of the system and slightly on the pressure of metal solid/metal liquid equilibration (Van Orman et al., 2008; Hayashi et al., 2009). This could be explained by the specific effects of each light elements on the iron phase diagram (melting temperature, solid liquid partitioning of the light element, liquid structure ...) (Boehler, 2000; Morard et al., 2008). So far, only one study on liquid–liquid exchange in the Fe–S–Si system has been done (Chabot et al., 2010), and no measurement has yet been performed for solid–liquid platinum group elements (PGEs) partitioning for the Fe–Si system, even though Si is likely to be present in the Earth's core.

In this study, we measured Si, Os, Re and Pt solid–liquid partition coefficients (D_{Si}, D_{Os}, D_{Re}, D_{Pt}) using a piston-cylinder apparatus. We reconstructed the melting loop at 2 GPa in the Fe–Si system and highlighted the effects of the underlying solid phase transitions on this melting loop. Correlations between liquid structures observed for Fe–Si liquid alloys, phase diagram properties and our partitioning results are established. We finally review the core–mantle interaction model (Brandon and Walker, 2005) in the light of our new data.

2. EXPERIMENTAL PROCEDURE

2.1. Ex situ partitioning experiments

The starting material consists of a mixture of high-purity powders (FeSi (99.9%, GoodFellow) Fe (99.99%, Alfa Aesar), Re (99.99%, Alfa Aesar), Pt (99.99%, Alfa Aesar), Os (99.99%, Alfa Aesar)). The PGE were added as 1 wt% of each, in order to obtain good quantitative measurements using electron microprobe analysis.

Experiments were performed at 2 GPa at temperatures between 1250 °C and 1600 °C using a 150-ton end-loaded piston-cylinder press. The 1/2″ cell assembly used in these experiments consisted in a MgO capsule, a graphite furnace and a talc/Pyrex or $BaCO_3$ pressure cell depending on temperature (Fig. 1). The temperature was raised at a rate of 100 °C per minute. The samples were quenched by shutting off the power supply to the furnace, resulting in a quench rate higher than 300 °C per second. The temperature was monitored using a type D thermocouple ($W_{97}Re_3$/$W_{75}Re_{25}$) inserted axially in an alumina four-bore thermocouple sleeve above the capsule. The melting loop in the Fe–Si is quite narrow, only few tens of degrees, therefore the sample was off-centered vertically with respect to the hotspot in order to impose a temperature gradient in the sample, and to have liquid/solid coexistence at a defined position (Fig. 1). Difference between solid and liquid was easily made using the dendritic texture of the liquid (Fig. 1). The experiment was run for 2 h in order to achieve complete equilibrium between the liquid and the solid. This duration was known to be sufficient, since the solid composition was homogeneous, at least in the 300 μm at the interface, where the chemical analyses were performed. In order to evaluate the temperature at the solid–liquid interface, we measured the temperature gradients throughout the capsule using this assembly configuration. We used the spinel growth technique detailed in (Watson et al., 2002) giving 20 °C/mm for talc Pyrex assemblies and 42 °C/mm for $BaCO_3$ assemblies.

2.2. Microprobe analysis

Chemical analyses of run products were performed using a Cameca SX100 microprobe at the Camparis facility. Wavelength-dispersive spectroscopy was adopted to measure the elements in this study (Fe, Si, O, Pt, Re, Os). The operating conditions were 15 kV and 10 nA, and counting time of 10 s on the peak and 10 s on background for major elements, and 30 s on peak and 10 s on background for trace elements. Pure metals Fe, Pt, Os together with FeSi, Fe_2O_3, and $LaReO_3$ were used as standards. As shown on Fig. 1, the liquid part of the sample shows a dendritic quench texture. Such a texture requires analyzing the chemical composition of a large area, rather than a point analysis. We used a defocused beam of ~20 μm to average the compositions of quenched texture. For our temperature conditions, the diffusion length is usually more than several hundreds of microns, even for two hour long experiments (Watson and Watson, 2003). Chemical analyses of the solid phase were performed over the first hundreds of microns

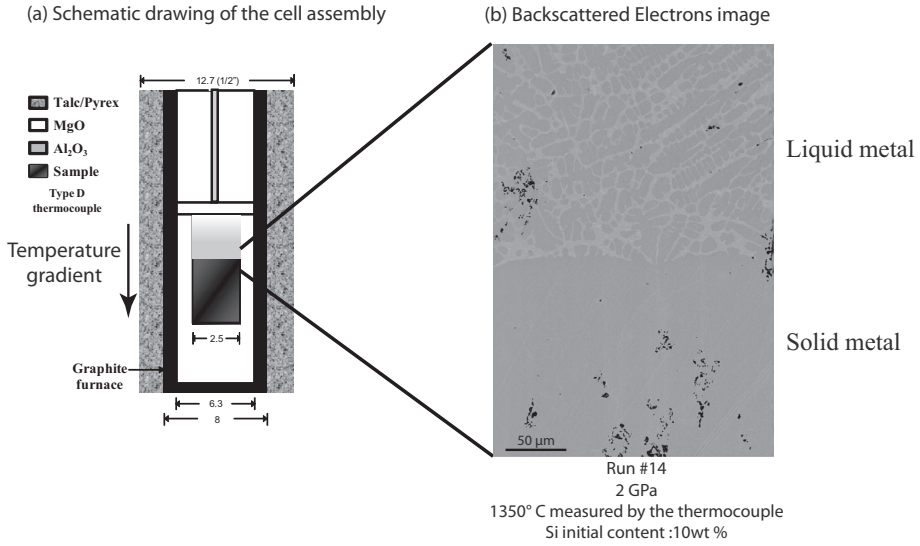

Fig. 1. (a) Schematic drawing of the piston-cylinder 1/2″ assembly. (b) Backscattered electron image of a recovered sample showing the coexistence of liquid and solid Fe–Si alloys. The liquid can easily be distinguished from the solid due to its dendritic quench texture. Dark features on the SEM image correspond to small SiO_2 grains crystallizing due to partial oxidation of silicon metal.

from the interface. This ensured that the measurements were taken on a sample at chemical equilibrium.

The Soret effect could potentially fractionate HSE elements through the liquid; however, this seems to be favored for S-bearing metallic liquids, but not for Si or C bearing metallic liquids (Brenan and Bennett, 2010). Furthermore, the robustness of our partitioning results is confirmed by the good agreement with pure Fe measured partitioning values (Chabot, pers. comm.).

3. RESULTS

In order to determine the phase diagram, we performed several experiments with varying initial Si content ranging from 3 wt% up to 12 wt%. This range of Si content is spans that recommended by various models of Earth's core composition (from 6 to 10 wt% Si) (Allègre et al., 1995; Javoy, 1995; McDonough, 2003; Badro et al., 2007; Antonangeli et al., 2010). The quench texture is similar for all of the samples, showing a dendritic liquid in the hottest part and a homogeneous solid in the coldest part. . The final silicon content of the samples after the equilibration experiment is usually slightly lower than the initial content, due to the formation of small SiO_2 grains, seen as black zones on backscattered images of the sample (Fig. 1). The temperature was set to right around melting, between 1600 °C and 1250 °C depending on Si concentration. The chemical analyses of each phase and the partition coefficient ($D^{sol/liq}$) of PGEs and Si between solid and liquid iron alloys are listed in Table 1.

The narrow melting loop on the Fe-rich side of the Fe–Si phase diagram has been estimated using the temperature at the solid–liquid interface and the chemical composition of the solid and liquid (Fig. 2 and Table 1). At 2 GPa, the melting temperature decreases continuously from 1610 °C for pure iron (Strong et al., 1973) to 1333 °C for a solid containing 9.7 (0.2) wt% Si. Then, an abrupt flattening in the melting slope occurs around 10 wt% Si (Fig. 2). This effect is related to phase transitions in the Fe–Si solid alloys, from the A2 disordered to the B2 ordered structure, as observed at ambient pressure (Meco and Napolitano, 2005). In the A2 structure, the Si atoms are randomly dispersed in the bcc lattice, substituting the Fe atoms (Lejček et al., 2007) whereas they have defined crystallographic sites in the B2 structure (CsCl-type structure). At ambient pressure, the disorder–order transition is favored by higher Si concentration as well as lower temperatures (Raghavan, 2003).

The disorder–order transition from A2 to B2 strongly affects Si partitioning between the solid and liquid (D_{Si}) (Fig. 2, inset). D_{Si} value evolves towards a minimum of 0.82 around 6 wt% Si in the liquid and remain constant up to ~10 wt% Si (A2–B2 transition in the solid). The strong dependence of D_{Si} on Si content in the liquid at 2 GPa is quite different from the calculated behavior under inner core conditions (Alfè et al., 2002). By calculating chemical potentials from ab initio simulations, this study shows no dependence of D_{Si} as a function of X_{Si}, which remains around unity up to 20 at% Si (~11 wt% Si).

The measured partition coefficients for PGEs between solid and liquid are constant over our range of Si concentrations. Only Pt partitioning shows a slight decrease for Si content above 8 wt%. Generally, PGE partition coefficients increase with increasing light element content in the liquid phase (Chabot et al., 2006, 2011). Furthermore, our results are in good agreement with recent results obtained in pure Fe (Chabot, pers. comm.) (Fig. 3).

4. DISCUSSION

The melting loop is strongly affected by the A2–B2 transition and this disorder–order transition (Fig. 2) modifies the Si partitioning coefficient D_{Si} from 0.86 to 0.97.

Table 1
Electron probe microanalyses of the quenched liquid and solid Fe–Si alloys in equilibrium. Run duration was 2 h for each experiment.

Run #	#41 ($BaCO_3$)	#40 ($BaCO_3$)	#24 (T/P)	#14 (T/P)	#21 (T/P)
Temperature (°C)	1650	1600	1450	1350	1340
ΔX (mm)[a]	1.7	1.8	1.7	0.9	1.3
T interface (°C)[b]	1580 (20)	1525 (20)	1417 (20)	1333 (20)	1314 (20)
Liquid phase					
Fe (wt%)	94.3 (0.5)	92.5 (0.5)	89.8 (0.6)	86.8 (0.5)	84.4 (1.5)
Si (wt%)	2.4 (0.5)	4.8 (0.3)	7.9 (0.1)	9.7 (0.2)	11.4 (0.2)
O (wt%)	0.2 (0.1)	0.3 (0.03)	0.2 (0.03)	–	0.3 (0.02)
Re (wt%)	1.1 (0.3)	1 (0.2)	1.1 (0.2)	1.2 (0.1)	1 (0.2)
Os (wt%)	1 (0.6)	1 (0.4)	1.1 (0.3)	1.3 (0.1)	0.8 (0.3)
Pt (wt%)	1.6 (0.5)	1.3 (0.2)	1 (0.1)	1.4 (0.1)	1.3 (0.1)
Tot	100.6 (0.4)	100.8 (0.4)	101.1 (0.8)	100.3 (0.5)	99.3 (1.5)
Solid phase					
Fe (wt%)	95 (1)	93 (0.2)	90.9 (0.9)	88.5 (0.4)	85.7 (1.7)
Si (wt%)	2.1 (0.2)	3.9 (0.1)	6.6 (0.1)	8.31 (0.1)	11.1 (0.1)
O (wt%)	0.1 (0.04)	0.2 (0)	0.2 (0.03)	–	0.3 (0.1)
Re (wt%)	1.4(0.2)	1.3 (0.1)	1.3 (0.3)	1.5 (0.1)	1.2 (0.2)
Os (wt%)	1.3 (0.2)	1.1 (0.1)	1.2 (0.2)	1.7 (0.2)	0.9 (0.3)
Pt (wt%)	1.3 (0.2)	1.2 (0.1)	0.7 (0.2)	0.9 (0.1)	0.6 (0.2)
Tot	101.2 (0.7)	100.7 (0.2)	100.9 (1)	100.8 (0.5)	99.9 (1.7)
D_{Re}	1.27 (0.4)	1.28 (0.3)	1.14 (0.34)	1.22 (0.14)	1.14 (0.3)
D_{Os}	1.27 (0.8)	1.1 (0.47)	1.09 (0.31)	1.28 (0.17)	1.13 (0.54)
D_{Pt}	0.78 (0.26)	0.89 (0.15)	0.73 (0.17)	0.63 (0.11)	0.47 (0.19)
D_{Si}	0.89 (0.19)	0.82 (0.06)	0.84 (0.01)	0.86 (0.02)	0.97 (0.02)

Partition coefficients are concentration (in weight) ratios between solid and liquid $D^{sol/liq}$.
[a] Distance between top of the sample and solid/liquid interface (ΔX).
[b] Temperature of the solid/liquid interface calculated after our cell assembly calibration (42 °C/mm for $BaCO_3$ pressure cell assembly and 20 °C/mm for talc/Pyrex cell assembly) following the method of spinel growth described in Watson et al. (2002).

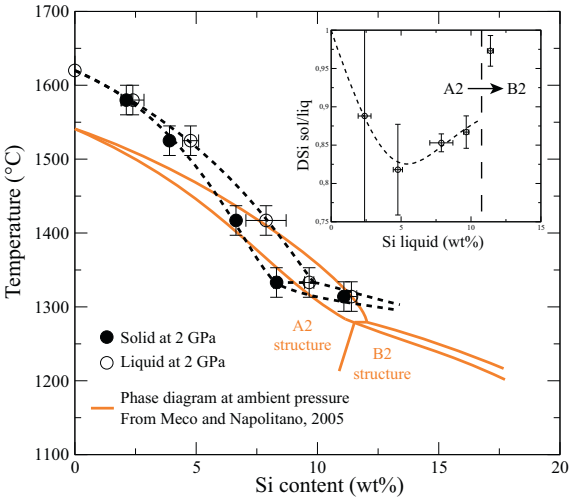

Fig. 2. Melting relations in the Fe–Si system at 2 GPa from our experiments and from Meco and Napolitano (2005). The change in the slope of solidus and liquidus observed around 10 wt% Si is related to disorder–order phase transitions in the surrounding solid. *Inset:* corresponding Si partitioning between solid and liquid D_{Si}.

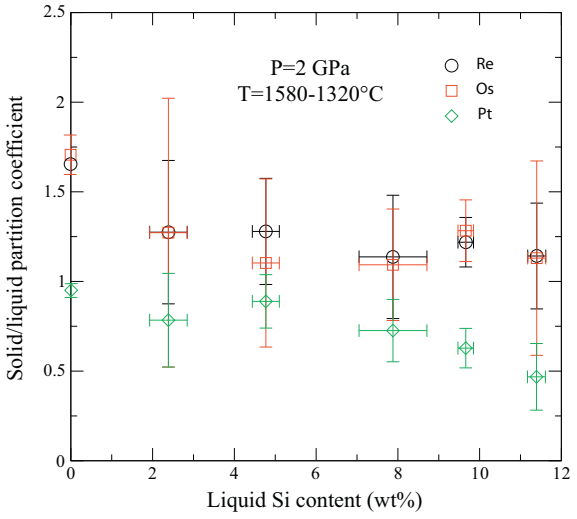

Fig. 3. Solid/liquid partition coefficient (C_i solid/C_i liquid in wt%) results for highly siderophile elements Re, Os and Pt obtained in the Fe–Si system. The partitioning of these elements shows no dependency on Si content. Values for solid/liquid partitioning in the case of pure Fe are from Chabot, pers. comm.

Ordering of the Si atoms in the B2 cell structure changes the solubility of Si in the solid phase. In fact, the presence of an ordered B2 phase at Earth's inner core P–T conditions is strongly debated. For an Si content lower than 7 wt% Si, only the hcp structure has been evidenced under Earth's core P–T conditions (Asanuma et al., 2011; Sakai et al., 2011) whereas above 9 wt% Si, a mixture of B2 and hcp structures could be stable at ICB conditions (Kuwayama et al., 2009; Fischer et al., 2013). The influence of the B2 phase on solid–liquid partitioning on ICB conditions could

lead to a maximum difference of 1.5 wt% between solid and liquid compositions with an Earth's core containing 7 wt% Si and even lower for higher Si content.

The density contrast at the ICB is usually estimated to be around 4.5%, from the PREM model (Dziewonski and Anderson, 1981), but could be significantly higher (up to 7%) for studies based on amplitudes of core reflected phases (Cao and Romanowicz, 2004). This observed density jump cannot solely be explained by the volume difference between the solid and the liquid (around 2% at ICB conditions) (Alfè et al., 2002). Therefore, the ICB density contrast has been ascribed to the segregation of light elements in the liquid outer core during inner core crystallization, which then drives compositional convection (Aubert et al., 2008; Hori et al., 2012). Using density values from Alfè et al. (2002), a Si enrichment in the liquid of 1–1.5 wt% leads to a density contrast of 3–3.5% at the ICB (breaking down as 2% for pure Fe solid/liquid density change and 1–1.5% due to preferential Si partitioning in the melt). Above 9 wt% Si in the Earth's core, Si stop contributing to the density contrast and we are left with the 2% from the solid/liquid density change in pure Fe. Therefore, the Fe–Si system could contribute to the ICB density jump for low Si concentration <7 wt%, yet at the same time it imposes that other light elements be present to account for the missing 1–4% density contrast.

In order to explain the observed Os isotopic anomaly in OIB lavas, the core-mantle exchange model requires large values for D_{Re} and D_{Os} (Brandon et al., 1998, 2003; Brandon and Walker, 2005). Depending on the core crystallization model used, the required values for D_{Re} range between 18 and 26 and D_{Os} between 28 and 44. The liquid outer core needs to be strongly enriched in non-radiogenic Os during inner core crystallization, and therefore inner core crystallization must be accompanied by a high D_{Os}/D_{Pt} (values over 10 in Brandon et al., 2003) (Fig. 4). This is clearly not the case in the Fe–Si system; we observe constant partition coefficients over the studied compositional range, with D_{Re} and D_{Os} ~1.2. We can also consider the Fe–S and Fe–C systems, which are potentially interesting for Earth's core (Poirier, 1994). These systems (Fig. 4) present similar trends, with D_{Os}/D_{Pt} between 1 and 3 for light element contents below 15 at%. For a higher light element content, this ratio could increase, especially for the Fe–S system, but will only reach the required value satisfying the model presented by Brandon et al. (2003) in the case of a S and C bearing liquid in equilibrium with solid Fe_3C (Fig. 4). This clearly demonstrates that the main requirement to satisfy the core–mantle interaction model (i.e. the low values of D_{Pt} compared to D_{Os} and D_{Re}) seems difficult to realize, irrespective of the considered Fe alloy system.

Multiple light elements could be present in the Earth's core; ternary systems, such as Fe–S–Si or Fe–S–C, become miscible under Earth's core pressure conditions (Corgne et al., 2008; Dasgupta et al., 2009; Morard and Katsura, 2010). However, since Si does not affect the partitioning of PGE compared to pure Fe, its addition to sulfur or carbon should not alter the PGE partitioning behavior observed in the binary systems. In fact, the only case where D_{Os}/D_{Pt} values are higher than 10 is for a Fe–S–C liquid in coexistence with solid Fe_3C (Buono et al., 2013). These values are relevant for an Earth's inner core composed of pure Fe_3C, but compatibility of Fe_3C sound velocity measured under high pressure with seismic observations is still debated (Fiquet et al., 2009; Gao et al., 2011).

Our experiments do not directly measure the solid/liquid partitioning of Si and highly siderophile elements Pt, Os, Re

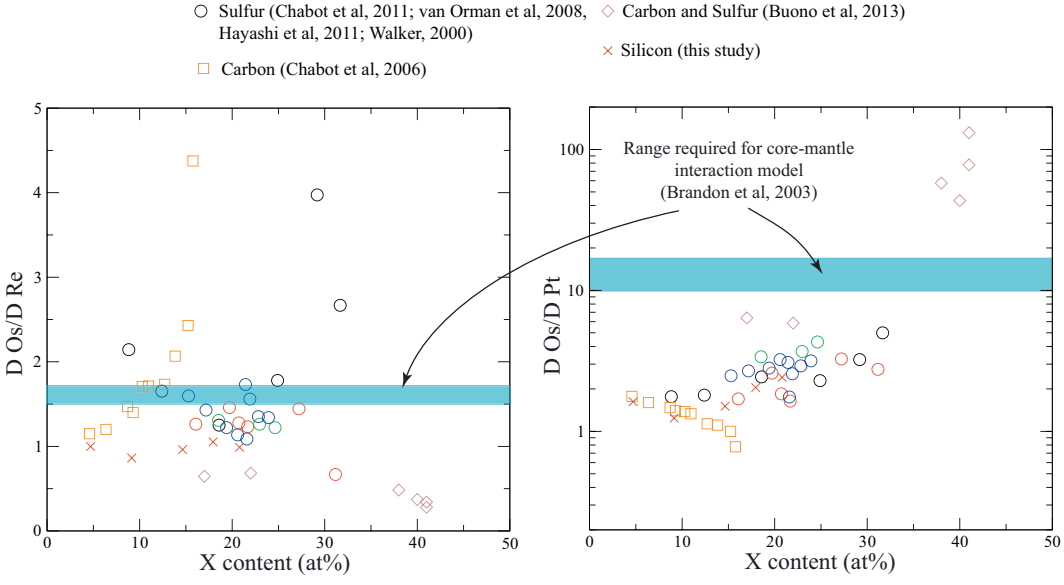

Fig. 4. Ratio of solid/liquid partition coefficients as a function of light element content in iron (Walker, 2000; Chabot et al., 2006, 2011; Van Orman et al., 2008; Hayashi et al., 2009; Buono et al., 2013). Similar behavior is observed for each PGE, with stronger effects of S rather than Si or C. For comparison, we indicate the values of DOs/DPt and DOs/DRe required to satisfy core mantle interaction model presented in Brandon et al. (2003).

at the conditions of the ICB. Extrapolations of our partitioning values up to ICB P–T conditions (330 GPa; ~6200 K, Anzellini et al., 2013) must take into account the structural evolution of solid and liquid iron alloys with pressure and light element composition (S, Si, C, O). At ambient pressure, the phase diagrams of Fe–S, Fe–Si and Fe–C alloys are drastically different, with a pure eutectic behavior for the Fe–FeS system to a solid solution behavior for the Fe–Si system (Kubaschewski, 1982). The small partitioning between solid and liquid in the Fe–Si system is a consequence of the compact structure of the Fe–Si liquid alloys, comparable to pure Fe up to 50 at% Si (Il'inskii et al., 2002; Morard et al., 2008). This liquid structure is compatible with the corresponding solid structure, explaining its high Si solubility, and also the constant partitioning of PGE from pure Fe up to 11 wt% Si. In contrast, S strongly affects the liquid structure, with a randomly packed structure for S content greater than 25 at% S (Siebert et al., 2004; Morard et al., 2008). This leads to the eutectic behavior in the Fe–FeS system, and the increase in partitioning values at high S content (Fig. 4). At pressures above 15 GPa, Fe–S liquid alloys evolve towards a compact structure (for S content above 25 at% S), similar to Fe–Si liquid alloys (Morard et al., 2007), while solubility of S in pure Fe increases with increasing pressure (Kamada et al., 2012). Therefore, PGE partitioning in the Fe–S system should decrease under Earth's core conditions, in agreement with what we observe for the Fe–Si system in this work. This suggests that the model of core-mantle exchange does not provide a plausible mechanism for producing a radiogenic Os isotopic signature in mantle plume-derived lavas, and that models implying mantle source heterogeneity (Meibom et al., 2002; Baker and Krogh Jensen, 2004; Luguet et al., 2008) should be favored.

5. CONCLUSION

The partitioning of PGE and Si between the solid and liquid in the Fe–Si system has been studied at a pressure of 2 GPa and temperatures ranging from 1340 to 1650 °C. The Fe–Si melting loop was found to be strongly affected by the order–disorder (A2–B2) transition, where the solubility of Si in the solid phase is enhanced by the ordering of Si atoms in B2-type structure. Furthermore, constant partition coefficients of PGEs have been observed over a wide range of Si concentrations in the liquid. Along with low values of these partition coefficients for S- and C-bearing systems, they are not compatible with the core–mantle interaction model (Brandon et al., 1998; Brandon and Walker, 2005) which attempts to explain the Os isotopic signature in OIBs as being the result of a core component.

ACKNOWLEDGMENTS

The research leading to these results has received funding from the European Research Council (ERC) under the European Community's Seventh Framework Programme (FP7/2007-2013)/ERC grant agreement 207467 and the PlanetLab program of French National Research Agency (ANR) Grant No. ANR-12-BS04-0015-04. We acknowledge the financial support of the UnivEarthS Labex program at Sorbonne Paris Cité (ANR-10-LABX-0023 and ANR-11-IDEX-0005-02). The authors thank M. Fialin at the Camparis analysis center (UPMC, IPGP, Paris). The original manuscript was improved by the constructive comments of R. Dasgupta, N.L. Chabot and two anonymous reviewers. We also thank Z. Reza for manuscript revision.

REFERENCES

Alfè D., Gillan M. J. and Price G. D. (2002) Composition and temperature of the Earth's core constrained by combining ab initio calculations and seismic data. *Earth Planet. Sci. Lett.* **195**, 91–98.

Allègre C. J., Poirier J. P., Humler E. and Hofmann A. W. (1995) The chemical composition of the Earth. *Earth Planet. Sci. Lett.* **134**, 515–526.

Antonangeli D., Siebert J., Badro J., Farber D. L., Fiquet G., Morard G. and Ryerson F. J. (2010) Composition of the Earth's inner core from high-pressure sound velocity measurements in Fe-Ni-Si alloys. *Earth Planet. Sci. Lett.* **295**, 292–296.

Anzellini S., Dewaele a., Mezouar M., Loubeyre P. and Morard G. (2013) Melting of iron at Earth's inner core boundary based on fast X-ray diffraction. *Science* **340**, 464–466.

Asanuma H., Ohtani E., Sakai T., Terasaki H., Kamada S., Hirao N. and Ohishi Y. (2011) Static compression of Fe0.83Ni0.09-Si0.08 alloy to 374 GPa and Fe0.93Si0.07 alloy to 252 GPa: implications for the Earth's inner core. *Earth Planet. Sci. Lett.* **310**, 113–118.

Aubert J., Amit H., Hulot G. and Olson P. (2008) Thermochemical flows couple the Earth's inner core growth to mantle heterogeneity. *Nature* **454**, 758–761.

Badro J., Fiquet G., Guyot F., Gregoryanz E., Occelli F., Antonangeli D. and D'Astuto M. (2007) Effect of light elements on the sound velocities in solid iron: implications for the composition of Earth's core. *Earth Planet. Sci. Lett.* **254**, 233–238.

Baker J. a. and Krogh Jensen K. (2004) Coupled ^{186}Os–^{187}Os enrichments in the Earth's mantle – core–mantle interaction or recycling of ferromanganese crusts and nodules? *Earth Planet. Sci. Lett.* **220**, 277–286.

Boehler R. (2000) High-pressure experiments and the phase diagram of lower mantle and core materials. *Rev. Geophys.* **38**, 221–245.

Brandon A. D. and Walker R. J. (2005) The debate over core-mantle interaction. *Earth Planet. Sci. Lett.* **232**, 211–225.

Brandon A. D., Walker R. J., Morgan J. W., Norman M. D., and Prichard H. M. (1998), Coupled ^{186}Os and ^{187}Os Evidence for Core-Mantle Interaction. Science (80-.). 280, 1570–1573.

Brandon A. D., Walker R. J., Puchtel I. S., Becker H., Humayun M. and Revillon S. (2003) ^{186}Os-^{187}Os systematics of Gorgona Island komatiites: implications for early growth of the inner core. *Earth Planet. Sci. Lett.* **206**, 411–426.

Brenan J. M. and Bennett N. (2010) Soret separation of highly siderophile elements in Fe–Ni–S melts: implications for solid metal–liquid metal partitioning. *Earth Planet. Sci. Lett.* **298**, 299–305.

Buono A. S., Dasgupta R., Lee C.-T. a. and Walker D. (2013) Siderophile element partitioning between cohenite and liquid in the Fe–Ni–S–C system and implications for geochemistry of planetary cores and mantles. *Geochim. Cosmochim. Acta* **120**, 239–250.

Cao A. and Romanowicz B. (2004) Constraints on density and shear velocity contrasts at the inner core boundary. *Geophys. J. Int.* **157**, 1146–1151.

Chabot N. L., Campbell A. J., Jones J. H., Humayun M. and Vern Lauer, Jr., H. (2006) The influence of carbon on trace element

partitioning behavior. *Geochim. Cosmochim. Acta* **70**, 1322–1335.
Chabot N. L., Safko T. M. and McDONOUGH W. F. (2010) Effect of silicon on trace element partitioning in iron-bearing metallic melts. *Meteorit. Planet. Sci.* **45**, 1243–1257.
Chabot N. L., McDonough W. F., Jones J. H., Saslow S. A., Ash R. D., Draper D. S. and Agee C. B. (2011) Partitioning behavior at 9 GPa in the Fe–S system and implications for planetary evolution. *Earth Planet. Sci. Lett.* **305**, 425–434.
Corgne A., Wood B. J. and Fei Y. (2008) C- and S-rich molten alloy immiscibility and core formation of planetesimals. *Geochim. Cosmochim. Acta* **72**, 2409–2416.
Dasgupta R., Buono A., Whelan G. and Walker D. (2009) High-pressure melting relations in Fe–C–S systems: implications for formation, evolution and structure of metallic cores in planetary bodies. *Geochim. Cosmochim. Acta* **73**, 6678–6691.
Day J. M. D., Pearson D. G., Macpherson C. G., Lowry D. and Carracedo J. C. (2010) Evidence for distinct proportions of subducted oceanic crust and lithosphere in HIMU-type mantle beneath El Hierro and La Palma, Canary Islands. *Geochim. Cosmochim. Acta* **74**, 6565–6589.
Dziewonski A. M. and Anderson D. L. (1981) Preliminary reference Earth model. *Phys. Earth Planet. Inter.* **25**, 297–356.
Fiquet G., Badro J., Gregoryanz E., Fei Y. and Occelli F. (2009) Sound velocity in iron carbide (Fe_3C) at high pressure: implications for the carbon content of the Earth's inner core. *Phys. Earth Planet. Inter.* **172**, 125–129.
Fischer R. A., Campbell A. J., Reaman D. M., Miller N. A., Heinz D. L., Dera P. and Prakapenka V. B. (2013) Phase relations in the Fe–FeSi system at high pressures and temperatures. *Earth Planet. Sci. Lett.* **373**, 54–64.
Gao L., Chen B., Zhao J., Alp E. E., Sturhahn W. and Li J. (2011) Effect of temperature on sound velocities of compressed Fe_3C, a candidate component of the Earth's inner core. *Earth Planet. Sci. Lett.* **309**, 213–220.
Hayashi H., Ohtani E., Terasaki H. and Ito Y. (2009) The partitioning of Pt–Re–Os between solid and liquid metal in the Fe–Ni–S system at high pressure: implications for inner core fractionation. *Geochim. Cosmochim. Acta* **73**, 4836–4842.
Hori K., Wicht J. and Christensen U. R. (2012) The influence of thermo-compositional boundary conditions on convection and dynamos in a rotating spherical shell. *Phys. Earth Planet. Inter.* **196**, 32–48.
Il'inskii A., Slyusarenko S., Slukhovskii O., Kaban I. and Hoyer W. (2002) Structural properties of liquid Fe-Si alloys. *J. Non-Cryst. Sol.* **306**, 90–98.
Javoy M. (1995) The integral enstatite chondrite model of the Earth. *Geophys. Res. Lett.* **22**, 2219–2222.
Kamada S., Ohtani E., Terasaki H., Sakai T., Miyahara M., Ohishi Y. and Hirao N. (2012) Melting relationships in the Fe–Fe_3S system up to the outer core conditions. *Earth Planet. Sci. Lett.* **359–360**, 26–33.
Kubaschewski O. (1982) *Iron-Binary Phase Diagrams*. Springer, Verlay, vol. 1.
Kutzner C. and Christensen U. (2000) Effects of driving mechanisms in geodynamo models. *Geophys. Res. Lett.* **27**, 29–32.
Kuwayama K., Sawai T., Hirose K., Sata N. and Ohishi Y. (2009) Phase relations of iron–silicon alloys at high pressure and high temperature. *Phys. Chem. Miner.* **36**, 511–518.
Lejček P., Hofmann S. and Janovec J. (2007) Prediction of enthalpy and entropy of solute segregation at individual grain boundaries of α-iron and ferrite steels. *Mater. Sci. Eng. A* **462**, 76–85.
Luguet A., Graham Pearson D., Nowell G. M., Dreher S. T., Coggon J. a., Spetsius Z. V. and Parman S. W. (2008) Enriched Pt-Re-Os isotope systematics in plume lavas explained by metasomatic sulfides. *Science* **319**, 453–456.
McDonough W. F. (2003) Compositional model for the Earth's core. *Treatise Geochem.* **2**, 547–568.
Meco H. and Napolitano R. E. (2005) Liquidus and solidus boundaries in the vicinity of order–disorder transitions in the Fe–Si system. *Scr. Mater.* **52**, 221–226.
Meibom A., Sleep N. H., Chamberlain C. P., Coleman R. G., Frei R., Hren M. T. and Wooden J. L. (2002) Re–Os isotopic evidence for long-lived heterogeneity and equilibration processes in the Earth's upper mantle. *Nature* **419**, 705–708.
Meibom A., Frei R. and Sleep N. H. (2004) Osmium isotopic compositions of Os-rich platinum group element alloys from the Klamath and Siskiyou Mountains. *J. Geophys. Res.* **109**, B02203.
Morard G. and Katsura T. (2010) Pressure temperature cartography of the Fe-S-Si immiscible system. *Geochim. Cosmochim. Acta* **74**, 3659–3667.
Morard G., Sanloup C., Fiquet G., Mezouar M., Rey N., Poloni R. and Beck P. (2007) Structure of eutectic Fe-FeS melts up to 17 GPa: implications for planetary cores. *Earth Planet. Sci. Lett.* **263**, 128–139.
Morard G., Sanloup C., Guillot B., Fiquet G., Mezouar M., Perrillat J. P., Garbarino G., Mibe K., Komabayashi T. and Funakoshi K. (2008) In situ structural investigation of Fe-S-Si immiscible liquid system and evolution of Fe-S bond properties with pressure. *J. Geophys. Res.* **113**, B10205.
Poirier J. P. (1994) Light elements in the Earth's outer core: a critical review. *Phys. Earth Planet. Inter.* **85**, 319–337.
Raghavan V. (2003) Fe-Ni-Si (iron-nickel-silicon). *J. Phase Equilibria* **24**, 269–271.
Sakai T., Ohtani E., Hirao N. and Ohishi Y. (2011) Stability field of the hcp-structure for Fe, Fe-Ni and FeNi-Si alloys up to 3 Mbar. *Geophys. Res. Lett.* **38**, L09302.
Schertsen A., Elliott T., Hawkesworth C. and Norman M. (2004) Tungsten isotope evidence that mantle plumes contain no contribution from the Earth's core. *Nature* **427**, 234–237.
Siebert J., Malavergne V., Guyot F., Combe R. and Martinez I. (2004) The behaviour of sulphur in metal-silicate core segregation under reducing conditions. *Phys. Earth Planet. Inter.* **143–144**, 433–443.
Siebert J., Badro J., Antonangeli D. and Ryerson F. J. (2013) Terrestrial accretion under oxidizing conditions. *Science* **339**, 1194–1197.
Strong H. M., Tuft R. E. and Hanneman R. E. (1973) The iron fusion curve and the γ-δ-liq triple point. *Met. Trans.* **4**, 2657–2661.
Takafuji N., Hirose K., Mitome M. and Bando Y. (2005) Solubilities of O and Si in liquid iron in equilibrium with (Mg, Fe)SiO_3 perovskite and the light elements in the core. *Geophys. Res. Lett.* **32**, L06313.
Van Orman J. a., Keshav S. and Fei Y. (2008) High-pressure solid/liquid partitioning of Os, Re and Pt in the Fe–S system. *Earth Planet. Sci. Lett.* **274**, 250–257.
Walker D. (2000) Core participation in mantle geochemistry: Geochemical Society Ingerson Lecture, GSA Denver, October 1999. *Geochim. Cosmichim. Acta* **64**, 2897–2911.
Watson H. C. and Watson E. B. (2003) Siderophile trace element diffusion in Fe–Ni alloys. *Phys. Earth Planet. Inter.* **139**, 65–75.
Watson E., Wark D., Price J. and Van Orman J. (2002) Mapping the thermal structure of solid-media pressure assemblies. *Contrib. Mineral. Petrol.* **142**, 640–652.

Associate editor: Rajdeep Dasgupta